Lipid Bilayers and Membrane Dynamics: Insight into Thickness Fluctuations

Andrea C. Woodka
NIST Center for Neutron Research, National Institute of Standards and Technology, Gaithersburg, Maryland 20899-6102, USA

Paul D. Butler
NIST Center for Neutron Research, National Institute of Standards and Technology, Gaithersburg, Maryland 20899-6102, USA and Department of Chemical & Biomolecular Engineering, University of Delaware, Newark, Delaware 19716, USA

Lionel Porcar and Bela Farago
Institut Laue Langevin, 6 rue Jules Horowitz, BP 156-38042, Grenoble Cedex 9, France

Michihiro Nagao*
NIST Center for Neutron Research, National Institute of Standards and Technology, Gaithersburg, Maryland 20899-6102, USA and Center for Exploration of Energy and Matter, Indiana University, Bloomington, Indiana 47408, USA
(Received 2 February 2012; published 31 July 2012)

Thickness fluctuations have long been predicted in biological membranes but never directly observed experimentally. Here, we utilize neutron spin echo spectroscopy to experimentally reveal such fluctuations in a pure, fully saturated, phosphocholine lipid bilayer system. These fluctuations appear as an excess in the dynamics of undulation fluctuations. Like the bending rigidity, the thickness fluctuations change dramatically as the lipid transition temperature is crossed, appearing to be completely suppressed below the transition. Above the transition, the relaxation rate is on the order of 100 ns and is independent of temperature. The amplitude of the thickness fluctuations is 3.7 Å ± 0.7 Å, which agrees well with theoretical calculations and molecular dynamics simulations. The dependence of the fluctuations on lipid tail lengths is also investigated and determined to be minimal in the range of 14 to 18 carbon tails.

DOI: 10.1103/PhysRevLett.109.058102 PACS numbers: 87.16.dj, 61.05.fg, 82.70.Uv

Biological membranes are supramolecular aggregates that harbor many chemical reactions essential to cellular function. They are self-assembled highly flexible structures that have the ability to undergo an array of dynamic conformational transitions which are vital to many biological processes. These motions range from individual lipid oscillation to the undulation of large (micron-size) patches of the membrane. At atomic to molecular length scales, the diffusion of individual lipids within the membrane has been shown to affect cell signal transduction [1], while at the large length scales membrane stiffness and fluidity have been shown to have a significant impact on cellular uptake and release [2]. The dynamics at intermediate length scales are fundamental to understanding how the large scale motions emerge from atomic and molecular movements and interactions, yet remain experimentally elusive. At this intermediate length scale, thickness fluctuations have been suggested theoretically [3–7] and even proposed as a mechanism for membrane pore formation [8,9]. The insertion and functioning of membrane proteins is believed to be heavily influenced by such dynamics [10]. Computational work has been done to evaluate the characteristic features of these fluctuations [11–14] with simulation snapshots clearly showing thickness fluctuations on the order of a few angstroms. While such fluctuations have never been experimentally observed in lipid membranes, they have been reported in the much more flexible surfactant membranes using neutron spin echo (NSE) spectroscopy [15,16]. Very recently, these fluctuations were investigated in more detail using an oil swollen surfactant system as a membrane mimic [17–19].

In this Letter, we report the experimentally measured thickness fluctuations in a single component phospholipid model membrane as a function of both lipid tail length and temperature. Unilamellar vesicles (ULVs) composed of a single lipid dimyristoyl, dipalmitoyl, or distearoyl phosphocholine (DMPC = 14 carbon double tails, DPPC = 16 carbons, or DSPC = 18 carbons) were prepared and their dynamics characterized using NSE complemented with small angle neutron scattering (SANS) and densitometry measurements to fully characterize each system.

DMPC, DPPC, and DSPC were purchased in both tail deuterated and fully hydrogenated forms from Avanti Polar Lipids. In order to highlight any thickness fluctuations, tail deuterated and fully hydrogenated lipids were mixed in an appropriate ratio so that the membrane tail region was contrast matched with D_2O. Saturated phosphocholine lipids undergo a first-order phase transition known as the melting transition temperature, T_m, resulting in a change in membrane thickness and density. T_m changes with deuteration and was determined for each lipid mixture by

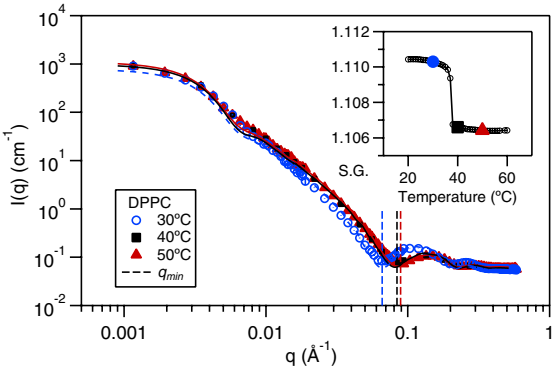

FIG. 1 (color online). SANS of DPPC vesicles (○) $T = 30\,^{\circ}\mathrm{C}$, (■) $T = 40\,^{\circ}\mathrm{C}$ (for clarity, only every 3rd data point is shown), and (▲) $T = 50\,^{\circ}\mathrm{C}$. Vertical lines represent $q_{\min}$. Fits are to the three shell vesicle model described. Inset: specific gravity of the DPPC sample as a function of temperature. Full symbols indicate temperatures where both SANS and NSE measurements were performed. Error bars represent ± 1 standard deviation and are smaller than the plotted data points.

measuring the specific gravity (see the inset of Fig. 1) as a function of temperature to be 20.5 °C, 37.5 °C, and 50.5 °C ($\pm$ 0.2 °C) for our DMPC, DPPC, and DSPC systems, respectively. The final system of relatively monodisperse lipid vesicles was prepared by heating each 10% lipid mass fraction solution above T_m and extruding through a 100 nm polycarbonate filter.

SANS data were collected at the National Institute of Standards and Technology (NIST) (on the NG3 and NG7 30 m SANS instruments) [20,21] and at the Institut Laue Langevin (ILL) (on D22). A $q[= 4\pi\lambda^{-1}\sin(\theta/2)]$ range of 0.001 to 0.45 Å^{-1} was investigated, where λ is the wavelength and θ is the scattering angle. The reduction of the SANS data was performed using NIST Center for Neutron Research (NCNR) developed macros [22] and ILL developed scripts (GRASansP) [23], while the analysis was performed using SansView [24].

NSE data were collected at NIST on the NG5-NSE [25,26] and at ILL on the IN15 spectrometers. Wavelengths of 6 and 8 Å were employed on NG5-NSE, while 6, 10, and 18 Å were used on IN15. The observed two-dimensional echo signal was treated to obtain the usual q-dependent normalized intermediate scattering function, $I(q, t)/I(q, 0)$ [27]. In this study, the relevant dynamics occur at the membrane thickness length scales, where the coherent scattering signal in the SANS profile is at a minimum. Thus, particular care must be taken in correcting for background.

Figure 1 shows the SANS from DPPC ULVs at 30 °C, 40 °C, and 50 °C. The scattering from the bilayer is modeled as vesicles with a Schulz distribution [28] of radii and composed of three layers, each with a corresponding scattering length density. The two outer layers of the membrane represent the hydrogenated lipid headgroup regions and were constrained to have equal thickness and scattering length density; the third (center) layer represents the deuterated lipid tail region. The lines in Fig. 1 represent the vesicle fits. The fit parameters for each lipid and temperature are summarized in Table I. The change in membrane thickness, d_m, on crossing T_m is clearly visible in the shift of the SANS dip position, $q_{\min}$.

The $I(q, t)/I(q, 0)$ data for each lipid were measured by NSE [see Fig. 2(a)]. Following the procedures used in the previous investigations for thickness fluctuations in surfactant membranes [17–19], a stretched exponential function with a stretching exponent of 2/3 was employed to fit the $I(q, t)/I(q, 0)$ data:

$$\frac{I(q, t)}{I(q, 0)} = \exp[-(\Gamma t)^{2/3}], \quad (1)$$

TABLE I. Fit parameters obtained from SANS results for each lipid and temperature. d_m, d_h, and d_t indicate the thicknesses of the entire, head only, and tail only regions of the membrane, respectively; $q_{\min}$ is the location of the SANS dip position. The error indicates one sigma for each fitting parameter.

Lipid	T(°C)	d_m (Å)	d_h (Å)	d_t (Å)	$q_{\min}$ (Å^{-1})
DMPC	15	55.6 ± 2.4	12.0 ± 0.4	31.6 ± 0.9	0.075 ± 0.007
	16	54.7 ± 1.9	12.3 ± 0.2	30.1 ± 0.9	0.078 ± 0.008
	25	49.9 ± 2.9	12.6 ± 0.7	24.8 ± 0.4	0.092 ± 0.005
	35	48.4 ± 2.2	12.6 ± 0.5	23.2 ± 0.5	0.095 ± 0.006
	35	48.1 ± 1.5	12.8 ± 0.2	22.6 ± 0.6	0.097 ± 0.008
DPPC	30	59.5 ± 3.7	11.4 ± 0.7	36.8 ± 0.3	0.066 ± 0.003
	40	52.1 ± 3.1	10.1 ± 0.6	31.8 ± 0.3	0.084 ± 0.003
	50	50.3 ± 3.0	10.1 ± 0.6	30.0 ± 0.3	0.089 ± 0.003
DSPC	45	60.7 ± 4.1	9.0 ± 0.6	42.7 ± 0.2	0.058 ± 0.007
	55	51.6 ± 3.3	9.5 ± 0.6	32.6 ± 0.2	0.076 ± 0.005
	65	49.8 ± 3.4	8.9 ± 0.6	32.0 ± 0.2	0.082 ± 0.007

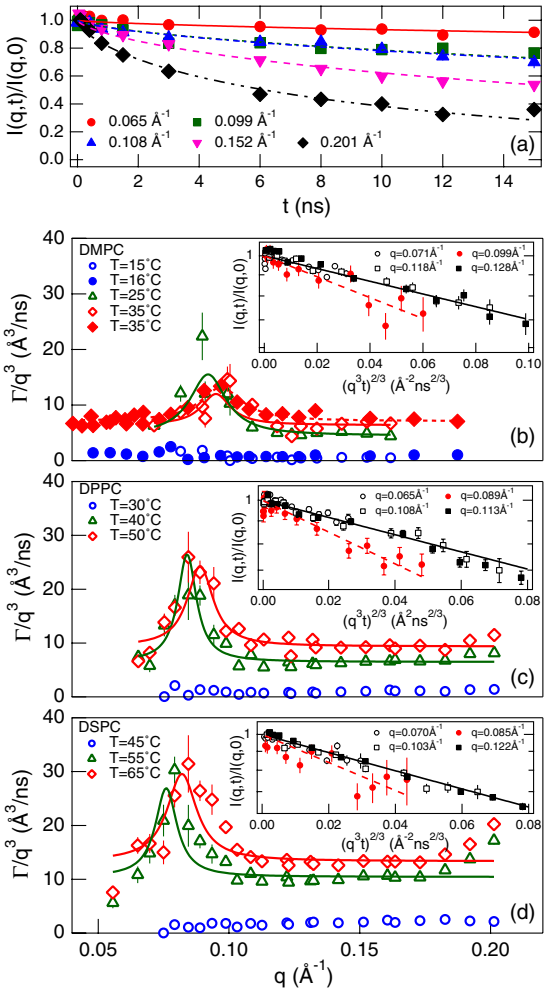

FIG. 2 (color online). (a) $I(q,t)/I(q,0)$ of DPPC vesicles at $T = 50\,^{\circ}\mathrm{C}$; fits are to Eq. (1). q dependence of Γ/q^3 for (b) DMPC, (c) DPPC, and (d) DSPC vesicles. Fits above T_m are to Eq. (4). Inset: plot of rescaled $I(q,t)/I(q,0)$ based on the theory of Zilman and Granek.

where Γ is the decay rate. In principle, the diffusion of the vesicles also contributes to the dynamics of the system. However, the diffusion constant for such a large object (vesicle radius ≈ 50 nm) of roughly 10^{-12} m^2/s, estimated from the Stokes-Einstein equation, is outside the NSE window. Thus, the theory of Zilman and Granek for the bending motion of a single membrane [29] should be applicable here and, as shown in previous studies of ULVs [30,31], Γ should scale as q^3.

As was the case for the previously studied surfactant system [17–19], the data for the fluid phase (above T_m) of the lipid systems shown in Figs. 2(b)–2(d) (DMPC, DPPC, and DSPC, respectively) clearly exhibit a deviation from the expected q^3 behavior, manifested as a peak in Γ/q^3. To further verify this deviation, we plot, as insets in Fig. 2, $I(q,t)/I(q,0)$ against the rescaled time $(q^3t)^{2/3}$. As expected, all the data fall on a master curve, except for the data at $q \approx 0.09$ Å^{-1}. This excess in dynamics is observed at the $q_{\min}$ observed in the SANS measurement (DPPC shown in Fig. 1, all values shown in Table I), indicating that the length scale of the enhancement in the dynamics signal is that of the membrane thickness. In the gel phase (below T_m), the lipid tails are much more ordered, leading to a much more rigid membrane which translates into the much smaller Γ observed here. Interestingly, in this regime there is no observable excess in the dynamics (peak in Γ/q^3). We note that, while a transition in the q dependence of Γ from q^3 at low q to q^2 for $q > 0.04$ Å^{-1} has been reported in ULVs [32] and attributed to a hybrid relaxation of the lipid bilayers, we observe no evidence for such a transition in any of our data. The only deviation we observe is the very localized excursion at q around 0.1 Å^{-1} (the membrane thickness) for temperatures above T_m, which registers as an enhancement rather than a suppression of the q dependence. Because of the lack of contrast in the plane of the bilayer on length scales within the q window, only motions perpendicular to the membrane are visible in such simple ULV systems. Thus, this excess in dynamics at the membrane thickness length scale must originate from thickness fluctuations.

In order to further characterize the excess in dynamics at the membrane thickness length scale, as in the previous work [17], we assume that the decay rate contains two additive terms and can be expressed by the following empirical equation:

$$\frac{\Gamma}{q^3} = \frac{\Gamma_{\mathrm{BEND}}}{q^3} + \frac{\Gamma_{\mathrm{TF}}}{q_0^3}\frac{1}{1+(q-q_0)^2\xi^{-2}}, \qquad (2)$$

where Γ_{BEND} indicates the decay rate due to the bending fluctuations and Γ_{TF} represents the decay rate due to the thickness fluctuations, leading to the excess dynamics observed at $q = q_0$. $\Gamma_{\mathrm{TF}}/q_0^3$ is the peak height of the Lorentzian, where q_0 is the peak position of the Lorentz function, and ξ^{-1} is the width of the Lorentzian [17]. According to the theory proposed by Zilman and Granek [29] and refined by Watson and Brown [33],

$$\Gamma_{\mathrm{BEND}} = 0.025\alpha\sqrt{\frac{k_{\mathrm{B}}T}{\tilde{\kappa}}}\frac{k_{\mathrm{B}}T}{\eta_{\mathrm{D_2O}}}q^3, \qquad (3)$$

where α is a factor close to unity originating from averaging the angle between the wave vector and a vector normal to the bilayer surface. $\eta_{\mathrm{D_2O}}$ is the viscosity of D_2O, k_{B} is Boltzmann's constant, and $\tilde{\kappa}$ is the effective bending modulus including the interlayer friction and is given by $\tilde{\kappa} = \kappa + 2d^2k_m$ [33], where d and k_m are the height of the neutral surface from the bilayer midplane and the monolayer lateral compressibility modulus, while κ is the intrinsic bending modulus. Although the value of d should be close to half the bilayer thickness, its exact value is not known. Thus, we employ the relation used for a similar lipid system of $2d/d_t = 1.21$ [30].

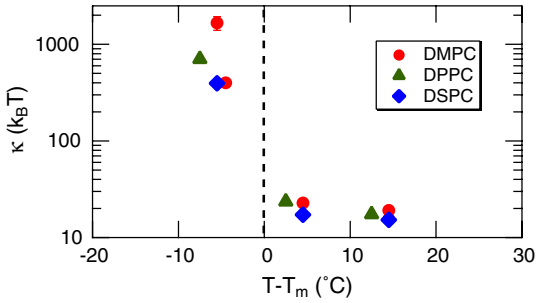

FIG. 3 (color online). The bending modulus, κ, plotted against the reduced temperature, $T - T_m$, for (●) DMPC, (▲) DPPC, and (◆) DSPC membranes.

Substituting Eq. (3) into Eq. (2) and using the expression $k_m = 24\kappa/d_t^2$ [34] yields

$$\frac{\Gamma}{q^3} = 0.0058\frac{k_B T}{\eta_{D_2O}}\sqrt{\frac{k_B T}{\kappa}} + \frac{\Gamma_{TF}}{q_0^3}\frac{1}{1+(q-q_0)^2\xi^{-2}}, \quad (4)$$

where η_{D_2O} and $k_B T$ are known quantities, while q_0 comes from the SANS measurements and α is set to 1. κ is plotted in Fig. 3 as a function of the reduced temperature, $T - T_m$. The expected transition in κ as T_m is crossed is clearly visible. The values of κ obtained in the fluid phase are approximately $20k_B T$ and within the uncertainty of our measurements are in agreement with the values found in the literature [30,35]. Note that, as both temperatures above T_m are also above the anomalous swelling regime, no softening of the bending modulus is expected.

The temperature dependence of the thickness fluctuation decay rates, Γ_{TF}, is shown in Fig. 4(a). Within our experimental uncertainty, these rates appear independent of either lipid tail length or temperature above T_m. The computed relaxation time, $\tau = 1/\Gamma_{TF}$, is on the order of 100 ns, much larger than the several nanoseconds estimated in surfactant membranes [15–19]. Such a significant slowdown of thickness fluctuation compared to those found in surfactant membrane systems might originate from larger membrane viscosities, increased membrane stiffness, or differences in compressibility of membranes. One explanation for the lack of observed thickness fluctuations below T_m is that if the decay times are slower (due, for example, to the higher bending rigidity) they will no longer be within the accessible experimental time window.

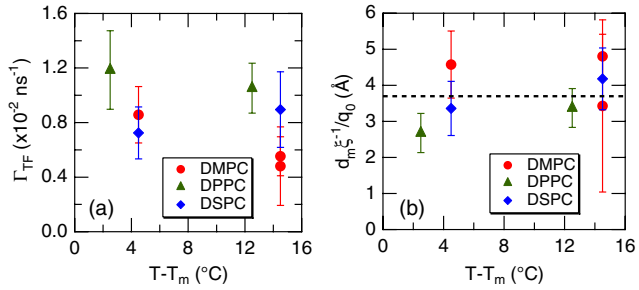

FIG. 4 (color online). Temperature dependence of (a) relaxation rate Γ_{TF} and (b) amplitude of thickness fluctuations $d_m\xi^{-1}/q_0$ (the dashed line is the average). (●) DMPC, (▲) DPPC, and (◆) DSPC.

The amplitudes of the thickness fluctuations are related to the observed peak width, ξ^{-1}, and can be estimated from $d_m\xi^{-1}/q_0$ [17–19]. As shown in Fig. 4(b), this value is also essentially independent of either tail length or temperature above T_m. The average thickness fluctuation amplitude was estimated to be 3.7 Å ± 0.7 Å, approximately 8% of the membrane thickness. This is not significantly smaller than the 12% found for surfactant membranes [18]. Thus, the amplitude appears to be controlled more by the bilayer's geometrical constraints, such as volume conservation, rather than dynamical ones. If this holds below T_m, then the lack of observed fluctuations would indeed be due to extremely slow relaxations.

The values of thickness fluctuation amplitude estimated here agree remarkably well with estimates based on both theory [6] and simulations [13,14]. The theory proposed by Huang for thickness fluctuations in lipid bilayers, based on the free energy of deformation, yields [6]

$$\langle D^2\rangle = \frac{k_B T}{\pi\kappa C_2}\left[\tan^{-1}\left\{\frac{(\frac{2\pi}{\lambda_0})^2 + C_1}{C_2}\right\} - \tan^{-1}\left(\frac{C_1}{C_2}\right)\right], \quad (5)$$

where $C_1 = \sigma/2d_m K_1$, $C_2 = \sqrt{4\bar{B}/d_m^2 K_1}$, and $K_1 = \kappa/d_m$. D is the thickness fluctuation amplitude, λ_0 is the cutoff wavelength ($\approx d_m/2$), $\bar{B}$ is the membrane normal compressibility coefficient, and σ is the half bilayer tension ($\approx$ surface tension). For each lipid and temperature, the bending moduli are obtained from our NSE measurements and the membrane thicknesses are determined from the SANS measurements, while the values for membrane compressibility and surface tension can be estimated from the literature [36–39]. In all cases, the result, $D \approx 4.5$ Å, is in very good agreement with the 3.7 Å ± 0.7 Å extracted from our experiments. Note that the theory predicts a similar amplitude even below T_m. This is only consistent with our data if the time scales for those fluctuations are outside our experimental window rather than being truly suppressed.

More recently, Lindahl and Edholm performed molecular dynamics simulations on a 10 to 60 ns time scale looking specifically at a fully hydrated DPPC bilayer in the fluid phase [13]. According to their simulations, the amplitude of the thickness fluctuation of a single DPPC (mono)layer is approximately 2.5 Å. The total thickness fluctuation amplitude, for the bilayer, would then be ≈ 5 Å, also in reasonable agreement with our results above T_m, albeit on a somewhat faster time scale than our 100 ns measured relaxation time.

An even more recent 8×10^6 step Monte Carlo simulation by West and Schmid [14], looking at the fluctuations and elastic properties of a DPPC lipid bilayer specifically in the

gel phase, reported a suppression of the thickness fluctuations. In particular, fluctuations in the tilt direction were of significantly smaller amplitude than in the fluid phase, while those in the direction perpendicular to the tilt were almost entirely suppressed. While clearly not conclusive, this result would tend to favor the interpretation of our data as being due to a true suppression of the mode rather than a simple slowdown moving it outside of the experimental window.

While these findings experimentally demonstrate the existence of thickness fluctuations in lipid membrane systems and provide some quantitative insights into them, there remains significant theoretical work on the physics of lipid bilayers in order to fully understand their dynamics. We hope that these findings will lead to other theoretical and experimental investigations of local intramembrane dynamics to improve our understanding of these interesting systems. In particular, the nature of the suppression remains an open question, as is the question of exactly how these fluctuations might enable pore formation, membrane protein insertion, or other biological functions.

This work utilized facilities supported in part by the National Science Foundation under Agreement No. DMR-0944772. This work benefited from DANSE software developed under NSF Grant No. DMR-0520547. Mention of any commercial products or services in this Letter does not imply approval or endorsement by NIST, nor does it imply that such products or services are necessarily the best available for the purpose.

*mnagao@indiana.edu

[1] D. Marguet, P. F. Lenne, H. Rigneault, and H. T. He, EMBO J. **25**, 3446 (2006).
[2] P. Weber, M. Wagner, W. S. L. Strauss, and H. Schneckenburger, Springer Proc. Phys. **114**, 372 (2007).
[3] D. Bach and I. R. Miller, Biophys. J. **29**, 183 (1980).
[4] S. B. Hladky and D. W. Gruen, Biophys. J. **38**, 251 (1982).
[5] I. R. Miller, Biophys. J. **45**, 643 (1984).
[6] H. W. Huang, Biophys. J. **50**, 1061 (1986).
[7] J. N. Israelachvili and H. Wennerstrom, J. Phys. Chem. **96**, 520 (1992).
[8] K. Kaufmann, W. Hanke, and A. Corcia, *Ion Channel Fluctuations in Pure Lipid Bilayer Membranes: Control by Voltage* (Caruaru, Brazil, 1989).
[9] L. Movileanu, D. Popescu, S. Ion, and A. I. Popescu, Bull. Math. Biol. **68**, 1231 (2006).
[10] R. B. Gennis, *Biomembranes: Molecular Structure and Function* (Springer, New York, 1989).
[11] E. G. Brandt and O. Edholm, J. Chem. Phys. **133**, 115101 (2010).
[12] G. Brannigan and F. L. H. Brown, Biophys. J. **90**, 1501 (2006).
[13] E. Lindahl and O. Edholm, Biophys. J. **79**, 426 (2000).
[14] B. West and F. Schmid, Soft Matter **6**, 1275 (2010).
[15] B. Farago, M. Monkenbusch, K. Goecking, D. Richter, and J. Huang, Physica (Amsterdam) **213–214B**, 712 (1995).
[16] B. Farago, Physica (Amsterdam) **226B**, 51 (1996).
[17] M. Nagao, Phys. Rev. E **80**, 031606 (2009).
[18] M. Nagao, S. Chawang, and T. Hawa, Soft Matter **7**, 6598 (2011).
[19] M. Nagao, J. Chem. Phys. **135**, 074704 (2011).
[20] C. J. Glinka, J. G. Barker, B. Hammouda, S. Krueger, J. J. Moyer, and W. J. Orts, J. Appl. Crystallogr. **31**, 430 (1998).
[21] S. M. Choi, J. G. Barker, C. J. Glinka, Y. T. Cheng, and P. L. Gammel, J. Appl. Crystallogr. **33**, 793 (2000).
[22] S. R. Kline, J. Appl. Crystallogr. **39**, 895 (2006).
[23] http://www.ill.eu/instruments-support/instruments-groups/groups/lss/grasp/.
[24] http://danse.chem.utk.edu.
[25] M. Monkenbusch, R. Schatzler, and D. Richter, Nucl. Instrum. Methods Phys. Res., Sect. A **399**, 301 (1997).
[26] N. Rosov, S. Rathgeber, and M. Monkenbusch, ACS Symp. Ser. **739**, 103 (1999).
[27] R. T. Azuah, L. R. Kneller, Y. M. Qiu, P. L. W. Tregenna-Piggott, C. M. Brown, J. R. D. Copley, and R. M. Dimeo, J. Res. Natl. Inst. Stand. Technol. **114**, 341 (2009).
[28] B. H. Zimm, J. Chem. Phys. **16**, 1099 (1948).
[29] A. G. Zilman and R. Granek, Phys. Rev. Lett. **77**, 4788 (1996).
[30] J. H. Lee, S. M. Choi, C. Doe, A. Faraone, P. A. Pincus, and S. R. Kline, Phys. Rev. Lett. **105**, 038101 (2010).
[31] Z. Yi, M. Nagao, and D. P. Bossev, J. Phys. Condens. Matter **21**, 155104 (2009).
[32] L. R. Arriaga, R. Rodríguez-García, I. López-Montero, B. Farago, T. Hellweg, and F. Monroy, Eur. Phys. J. E **31**, 105 (2010).
[33] M. C. Watson and F. L. H. Brown, Biophys. J. **98**, L9 (2010).
[34] W. Rawicz, K. C. Olbrich, T. McIntosh, D. Needham, and E. Evans, Biophys. J. **79**, 328 (2000).
[35] C. H. Lee, W. C. Lin, and J. Wang, Phys. Rev. E **64**, 020901(R) (2001).
[36] W. Schrader, H. Ebel, P. Grabitz, E. Hanke, T. Heimburg, M. Hoeckel, M. Kahle, F. Wente, and U. Kaatze, J. Phys. Chem. B **106**, 6581 (2002).
[37] L. N. Okoro, Int. J. Chem. **3**, 166 (2011) [http://www.ccsenet.org/journal/index.php/ijc/article/view/9299/6855].
[38] S. Halstenberg, T. Heimburg, T. Hianik, R. Kaatze, and R. Krivanek, Biophys. J. **75**, 264 (1998).
[39] A. Vrij, J. G. H. Joosten, and H. M. Fijnaut, Adv. Chem. Phys. **48**, 329 (1981).